(49) Zaloudek, F.; Novros, J. S.; Clark, L. B. J. Am. Chem. Soc. 1985, 107, 7344-7351.
(50) Bott, C. C.; Kurucsev, T. Spectrosc. Lett. 1977, 10, 495-499.
(51) Imabuko, K. J. Phys. Soc. Jpn. 1968, 24, 143-151.
(52) The dipole moment vector is defined herein as pointing from negative to positive. Note that the reverse convention is used for cytosine in ref 34.
(53) Kulakowska, I.; Geller, M.; Lesyng, B.; Wierzchowski, K. L. Biochim. Biophys. Acta 1974, 361, 119-130.
(54) Eisenstein, M. Int. J. Quantum Chem. 1988, 33, 127-158.
(55) Mulliken, R. S. J. Chem. Phys. 1955, 23, 1833-1840.
(56) Kulakowska, I.; Geller, M.; Lesyng, B.; Bolewska, K.; Wierzchowski, K. L. Biochim. Biophys. Acta 1975, 407, 420-429.

Isotropic Chemical Shifts and Quadrupolar Parameters for Oxygen-17 Using Dynamic-Angle Spinning NMR

K. T. Mueller,† J. H. Baltisberger, E. W. Wooten,‡ and A. Pines*

Materials Sciences Division, Lawrence Berkeley Laboratory, 1 Cyclotron Road, Berkeley, California 94720, and Department of Chemistry, University of California, Berkeley, California 94720 *(Received: April 9, 1992)*

Several oxygen-17-enriched silicates were studied using dynamic-angle spinning (DAS) NMR spectroscopy at two magnetic field strengths. The DAS method averages second-order quadrupolar interactions by reorienting a sample about a time-dependent axis, thereby yielding high-resolution spectra for half-odd integer spin quadrupolar nuclei such as oxygen-17. A narrow spectral line is observed for each distinct oxygen site in a powdered sample at the sum of the isotropic chemical shift and the field-dependent isotropic second-order quadrupolar shift. Using equations for the total shift observed at two field strengths, the chemical shift is uniquely determined together with a product of the quadrupolar coupling constant ($C_Q = e^2qQ/h$) and the quadrupolar asymmetry parameter (η). For one silicate, we demonstrate a computer program that uses the isotropic shifts and quadrupolar products as constraints and provides simulations of overlapped magic-angle spinning line shapes. In this way the quadrupolar parameters, C_Q and η, are determined separately for each crystallographic site. The silicates studied include the discrete orthosilicates larnite (Ca_2SiO_4) and forsterite (Mg_2SiO_4), as well as diopside ($CaMgSi_2O_6$), wollastonite ($CaSiO_3$), and clinoenstatite ($MgSiO_3$), which are minerals composed of chains of silicon–oxygen tetrahedra.

Introduction and Theory

Oxygen is a major constituent of many important compounds, including minerals, zeolites, glasses, proteins, and nucleic acids. The properties and functions of these materials are intimately tied to their microscopic structure.[1-5] Solid-state nuclear magnetic resonance (NMR) spectroscopy is a sensitive and isotopically selective probe of bonding and local microstructure and a potentially powerful tool for the study of microscopic oxygen environments in the solid state. Unfortunately, the only NMR active isotope of oxygen is oxygen-17 ($I = {}^5/_2$), which has a low natural abundance (0.037%). This, together with the large quadrupolar interaction experienced by oxygen-17 in many solids, makes observation and interpretation of oxygen-17 NMR spectra difficult. Oldfield and co-workers have studied zeolites,[6,7] minerals,[8,9] transition-metal carbonyls,[10] and simple oxides,[11-13] with high-resolution NMR techniques such as magic-angle spinning (MAS) NMR. More recently, oxygen-17 has been used as a probe of local environments and spin dynamics in magnetically ordered high-T_c superconducting oxides.[14,15] The dynamic motion of oxygen atoms in solids can also be discerned through relaxation rate measurements, either directly from oxygen-17 nuclei in isotopically enriched samples[16] or indirectly through the study of proton relaxation in the rotating frame.[17]

For many solids, especially those composed of microcrystalline or amorphous structures, resonances from distinct oxygen sites take the form of broad lines which may overlap and complicate analysis. For the readily observed central spin transition ($+{}^1/_2 \leftrightarrow -{}^1/_2$) in nuclei with half-odd integer spin, the principal broadening arises from the first-order chemical shift and second-order quadrupolar interactions. While the chemical shift anisotropy (CSA) is typically removed by MAS,[18-20] the quadrupolar broadening cannot be fully removed by spinning about any single spatial axis. Spinning at angles other than the magic angle (54.74°) can sometimes provide narrowing of the spectral lines,[21-24] but CSA and quadrupolar broadening still contribute to these line shapes. The techniques of dynamic-angle spinning (DAS) and double rotation (DOR) were developed to overcome the broadening induced by these (and other) anisotropies.[25-28] Resolved spectral lines have been obtained for boron-11,[29] sodium-23,[27,30] oxygen-17,[27,31,32] aluminum-27,[33-35] and rubidium-87[36] nuclei with these techniques.

The total isotropic shift (δ_{obs}) observed for a resonance in DAS (or DOR) is the sum of two isotropic components:

$$\delta_{obs} = \delta_{iso}^{(CS)} + \delta_{iso}^{(2Q)} \quad (1)$$

where the first term is the isotropic chemical shift and the second is the isotropic second-order quadrupolar shift. The chemical shift (in ppm) is field-independent and equal to one-third of the trace of the chemical shift tensor. For a nucleus with spin I, the isotropic quadrupolar shift of the central transition is

$$\delta_{iso}^{(2Q)} = -\frac{3}{40}\left(\frac{C_Q}{\nu_L}\right)^2 \frac{(I(I+1) - 3/4)}{I^2(2I-1)^2}\left(1 + \frac{\eta^2}{3}\right) \times 10^6 \quad (2)$$

with the quadrupolar coupling constant defined as

$$C_Q \equiv e^2qQ/h \quad (3)$$

and ν_L the Larmor frequency of the nucleus. The quadrupolar asymmetry parameter (η) describes the deviation of the local electric field gradient from cylindrical symmetry, while the quadrupolar coupling constant reflects the magnitude of the gradient. Note that in the slow-motion limit this total shift of the center of gravity of the NMR resonance occurs in all conventional high-field NMR spectra of solids including those from static sample experiments, MAS or variable-angle spinning experiments, and with the newer techniques of DAS and DOR. With DAS and DOR, however, the lines are narrowed and the maxima of the resonances occur at the positions of the total isotropic shifts for each magnetically inequivalent species.

Since the isotropic second-order quadrupolar shift is inversely proportional to the square of ν_L, the contributions of $\delta_{iso}^{(CS)}$ and $\delta_{iso}^{(2Q)}$ to the total shift can be determined by performing DAS experiments in magnetic fields of different strengths. The isotropic

† Present address: Department of Chemistry, University of British Columbia, Vancouver, BC V6T 1Z1.
‡ Present address: Biophysics Research Division, The University of Michigan, Ann Arbor, MI 48109-2099.
* To whom correspondence should be addressed.

0022-3654/92/2096-7001$03.00/0

chemical shift and the quadrupolar product for each site

$$P_Q \equiv C_Q\sqrt{(1 + \eta^2/3)} \quad (4)$$

can be calculated directly by solving a set of simultaneous equations as described below.

We have exploited the field dependence of the DAS spectra of oxygen-17 to uniquely determine values for the isotropic chemical shifts experienced at crystallographically distinct oxygen sites in several silicate minerals. Determination of the second-order quadrupolar shift, and hence P_Q, also allows an approximate calculation of C_Q at each site since the parameter η must lie between 0 and 1. In other words, the value of C_Q is bounded from above by P_Q and below by approximately 0.87 P_Q. Examination of the experimentally determined parameters reveals interesting trends in the values consistent with earlier reports and especially useful for predictive analysis of local microstructure.

Computer simulations of MAS line shapes at two field strengths using the isotropic shift data obtained from DAS experiments are possible. By fixing the values of the isotropic chemical shift and the quadrupolar product, simulations rapidly converge on best-fit values for the individual quadrupolar parameters C_Q and η at each type of oxygen site. We have carried this out for the three crystallographically inequivalent oxygens in the mineral diopside.

Experimental Section

Materials. The oxygen-17-labeled mineral samples were prepared by Stebbins and co-workers following a procedure reported previously.[32,37] Diopside was uniformly enriched with oxygen-17 to 20%, while all other samples were 40% labeled. The phase identities and stoichiometry of these materials were analyzed using silicon-29 NMR, and the findings were confirmed by powder X-ray diffraction. The forsterite sample was contaminated with approximately 25% clinoenstatite, but this did not affect the final NMR measurements significantly. Unit-cell structures have been reported previously for diopside,[38] forsterite,[39] clinoenstatite,[40] wollastonite,[41] and larnite.[42] They contain three, three, six, nine, and four crystallographically distinct oxygen sites, respectively.

NMR Measurements. NMR spectra were recorded at 9.4 and 11.7 T in standard wide-bore magnet systems. The DAS probes used for these experiments were home built using a design detailed in ref 34. MAS spectra were obtained using the same probe with the spinning angle fixed with respect to the magnetic field at 54.74°.

In a DAS experiment, spin evolution must occur at *two different* spinning angles of the sample rotor in order for broadening from both the quadrupolar and chemical shift anisotropies to vanish. An experiment with equal evolution times at the two angles was chosen to simplify the data collection. In this experiment, we rotate the sample first about $\theta_1 = 37.38°$ and then about, $\theta_2 = 79.19°$. At the completion of the spin evolution at the second angle the magnetization refocuses into a spin echo which has effectively precessed with an isotropic shift (see eq 1) as a function of the full evolution time. The usual hopping time between these two angles ranged from 25 to 35 ms, which was significantly shorter than the T_1 relaxation times for oxygen-17 in these compounds. The DAS pulse sequence and phase cycle used to collect the data were the same in previous experiments.[27] The radio-frequency pulse widths were calibrated to excite selectively only the central transition of oxygen-17[43,44] and were typically in the range 4–6 μs for $\pi/2$ pulses (equivalent to solution flip angles of $\pi/6$). A recycle delay of 1 or 2 s allowed the magnetization to relax to thermal equilibrium with the lattice. In addition, the experiment for data collected at 11.7 T used a modified sequence which had a π pulse inserted after the final $\pi/2$ pulse, at a time $\tau_r = 1/\nu_r$, to again refocus the DAS echo while shifting this echo by an additional rotor period. Spinning rates (ν_r) were typically between 6 and 7 kHz. This effectively removes receiver dead time and ringing effects from the final one-dimensional DAS spectra.

All one-dimensional DAS spectra were collected by sampling the complex signal intensity of the DAS echo for each of a series of evolution times. The interferograms were Fourier transformed and phased to produce DAS spectra with an overall sweep width of $1/\Delta t$, where Δt is the increment in the evolution period. We usually sampled between 128 and 512 time points which provides digital resolution of approximately 0.5 ppm. All oxygen-17 peaks were referenced to an external sample of $H_2{}^{17}O$ (37% enriched) in a small ampule placed inside an otherwise empty DAS sample rotor.

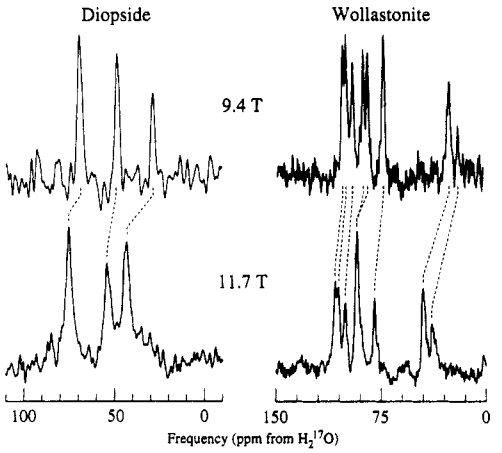

Figure 1. Dynamic-angle spinning (DAS) NMR spectra of oxygen-17 nuclei in two silicates, diopside ($CaMgSi_2O_6$) and wollastonite ($CaSiO_3$), at magnetic field strengths of 9.4 and 11.7 T.

Computer Simulations. Computer simulations were performed on a Stardent 750 computer using a program which calculates second-order quadrupolar powder patterns for samples spinning about any single axis. This program simulates only the central transition for half-odd integer nuclei and ignores intensity displaced into spinning side bands. It utilizes a simple and efficient technique for averaging over the orientations found within a powder.[45] The inputs to the program are the chemical shifts and the quadrupolar parameters for each oxygen site. We chose to simulate magic-angle spinning data so that it is possible to ignore first-order chemical shift anisotropy in the spectra. The experimental spectra were fit using an AMOEBA simplex routine,[46] allowing rapid convergence of parameters by minimizing the root-mean-square deviation between the simulated and the experimental spectra. Each fit takes approximately 2000 iterations, with each iteration requiring approximately 0.4 s per powder pattern. By using the quadrupolar product and isotropic chemical shift values determined directly from the one-dimensional DAS spectra, we are able to fix two parameter values for each site, limiting the simplex to only four variable parameters for each type of oxygen environment: the quadrupolar asymmetry parameter (η), the total intensity of the resonance line, a Lorentzian broadening factor, and a Gaussian broadening factor. By fitting MAS spectra at both 9.4 and 11.7 T, we place an even larger number of constraints on our simulations. Thus the asymmetry parameters and the quadrupolar coupling constants are determined with more reliability than parameters from fits of overlapping powder patterns (say from three oxygen sites as in diopside) but without the constraints provided by the DAS data.

Results and Discussion

The field-dependence of the resonances observed in oxygen-17 DAS NMR is demonstrated for the polycrystalline minerals diopside and wollastonite in Figure 1. Crystallographically inequivalent oxygen sites give rise to one narrow line each in the DAS spectra at both 9.4 and 11.7 T. As field strength increases, the total isotropic shift (in ppm) must move to a higher frequency since the isotropic chemical shift remains the same and the isotropic second-order quadrupolar shift is less negative (see eq 2). Inspection of the oxygen resonances in Figure 1 shows that the lines have not unexpectedly crossed at an intermediate value of the field. Care must be exercised, however, in more complex systems where additional studies at other field strengths or careful analysis of two-dimensional DAS line shapes may be required to determine whether resonances have crossed. When CSA is small, the anisotropic powder patterns in the second DAS dimension will

TABLE I: Results from Performing DAS Experiments at 9.4 and 11.7 T[a]

compd	$\delta_{obs}^{9.4T}$ (ppm)	$\delta_{obs}^{11.7T}$ (ppm)	$\delta_{iso}^{(CS)}$ (ppm)	$C_Q(1+\eta^2/3)^{1/2}$ (MHz)
diopside	69.2	75.1	86	2.8 ± 0.2
($CaMgSi_2O_6$)	48.5	54.0	64	2.7 ± 0.2
	28.6	43.3	69	4.5 ± 0.1
forsterite	49.0	57.1	72	3.3 ● 0.1
(Mg_2SiO_4)	49.0	54.8	64	2.8 ● 0.2
	30.8	37.5	49	3.0 ± 0.2
clinoenstatite	39.3	45.5	57	2.9 ± 0.2
($MgSiO_3$)	34.5	44.1	61	3.6 ● 0.1
	32.3	42.0	59	3.6 ● 0.1
	26.3	39.0	62	4.2 ± 0.1
	18.0	36.8	70	5.1 ± 0.1
	15.0	34.7	70	5.2 ± 0.1
wollastonite	103.4	107.4	115	2.3 ● 0.2
($CaSiO_3$)	100.1	105.1	114	2.6 ● 0.2
	96.5	100.2	107	2.2 ● 0.2
	89.0	91.9	97	2.0 ± 0.2
	85.8	91.9	103	2.9 ± 0.2
	74.3	79.3	88	2.6 ± 0.2
	28.2	44.9	75	4.8 ± 0.1
	28.2	44.9	75	4.8 ● 0.1
	21.6	37.8	67	4.7 ● 0.1
larnite	117.3	123.3	134	2.9 ± 0.2
(Ca_2SiO_4)	113.3	118.5	128	2.7 ● 0.2
	108.8	113.4	122	2.5 ± 0.2
	106.3	112.0	122	2.8 ● 0.2

[a] The isotropic chemical shifts and products of quadrupolar parameters were calculated from eqs 5 and 6. Errors in the measured total shifts at both field strengths are ±0.5 ppm, providing an isotropic chemical shift error of ±2 ppm for all calculated values.

be similar, yet scaled, for the same site at different field strengths. A modification of the DAS experiment,[47] utilizing a second hop to finish each isotropic evolution at the magic angle, overcomes any difficulties with CSA in the broadened second dimension and separated MAS line shapes are obtained directly.[36]

The total observed isotropic shifts in the DAS spectra of diopside, wollastonite, and the three other silicates are compiled in Table I. Substituting the relevant constants for oxygen-17 and the two field strengths into eq 1 yields the following set of simultaneous equations:

$$\delta_{obs}^{9.4T} = \delta_{iso}^{(CS)} - 2.03691P_Q^2 \quad (5)$$

$$\delta_{obs}^{11.7T} = \delta_{iso}^{(CS)} = 1.30476P_Q^2 \quad (6)$$

The shift values are all in units of ppm while P_Q is given in megahertz. The set of equations may be solved for $\delta_{iso}^{(CS)}$ and P_Q, and the results are shown at the right in Table I. The errors in calculating the isotropic chemical shifts (±2 ppm for all reported values) are much larger than the errors in the total shifts obtained directly from the DAS spectra since only two data points have been recorded per site.

The diopside data in Table I were used to place constraints upon the simulations of MAS line shapes at both field strengths. The calculated line shapes are compared to the original MAS spectra in Figure 2. The best-fit quadrupolar parameters and the isotropic chemical shift for each site are compiled in Table II, where they are compared with previously determined values.[9]

In the three chain silicates studied (diopside, clinoenstatite, and wollastonite), the occupancy of terminal oxygen sites in the structure is twice that of bridging oxygen species. In forsterite and larnite, all oxygen sites are nonbridging. Diopside, clinoenstatite, and wollastonite have three, six, and nine crystallographically distinct oxygen sites, respectively, and therefore one, two, and three different bridging sites. Referring to Table I, we note that the quadrupolar products P_Q for the oxygen sites in the chain silicates are predominantly less than 4 MHz. Values higher than 4.3 MHz follow a 1:2:3 ratio respectively for diopside, clinoenstatite, and wollastonite, suggesting that lines associated with these values should be assigned to bridging sites. This observation is compatible with the results of Oldfield and co-workers in their

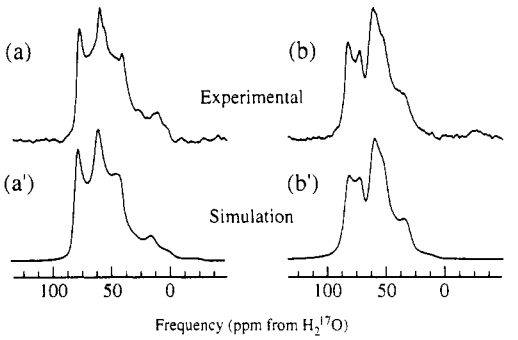

Figure 2. (a) Experimental magic-angle spinning (MAS) spectrum of oxygen-17 in diopside at 9.4 T. (a') Simulated spectrum at 9.4 T using parameters in Table II. (b) Experimental magic-angle spinning (MAS) spectrum of oxygen-17 in diopside at 11.7 T. (b') Simulated spectrum at 11.7 T using parameters in Table II.

TABLE II: Results from MAS Simulations at 9.4 and 11.7 T[a]

	this study			previous study (ref 9)		
site	$\delta_{iso}^{(CS)}$ (ppm)	C_Q (MHz)	η	$\delta_{iso}^{(CS)}$ (ppm)	C_Q (MHz)	η
1	86	2.83 ± 0.05	0.13 ± 0.10	84	2.7	0.0
2	64	2.74 ± 0.05	0.00 ± 0.10	63	2.7	0.1
3	69	4.39 ± 0.05	0.36 ± 0.05	69	4.4	0.3

[a] The constraints imposed on the results were fixed values of the isotropic chemical shift and the quadrupolar product, $P_Q = C_Q(1+\eta^2/3)^{1/2}$.

studies of these and similar silicates.[9] The DAS technique now allows complete resolution of all sites, even in wollastonite. For this silicate with nine crystallographic oxygen sites, the NMR data now reveal six distinct terminal sites as well as two inequivalent bridging sites occurring in a 2:1 ratio.

A number of trends are conspicuous when the isotropic chemical shifts for the various types of oxygen sites are examined. All of the bridging sites have isotropic chemical shifts within 4 ppm of 71 ppm, referenced to the oxygen-17 resonance from $H_2{}^{17}O$. This is an extremely small deviation considering the wide range of chemical shifts reported for oxygen-17.[48] Here, however, all of the oxygen sites are quite similar and differ only in the identities of neighboring cations. As noted by Oldfield and co-workers,[9] the chemical shifts of the bridging oxygens is generally less sensitive to the nature of the nearby cations due to the distance separating the oxygen nuclei and the cations.

Chemical shifts of Si–O terminal sites are more strongly dependent on the cations present. The deshielding of the oxygen nucleus as the effective ionic radius increases has been established empirically[9] and when the cations are magnesium ions (as in forsterite and clinoenstatite), the isotropic chemical shifts calculated range between 49 and 72 ppm. When calcium ions are present exclusively (wollastonite and larnite), the isotropic chemical shifts for the 10 sites lie between 88 and 134 ppm. In the mixed cation compound (diopside), both terminal oxygen sites had intermediate chemical shift values (64 and 88 ppm). Thus it appears that each oxygen in diopside experiences an averaged chemical shift value from the surrounding cations.

Similar trends are also observed when the quadrupolar coupling products are examined. For the bridging sites, P_Q values range between 4.5 and 5.2 MHz. This again is a very small range considering that oxygen-17 coupling constants as large as 12 MHz are observed for similar sites.[49] For the terminal sites in the magnesium-containing minerals P_Q values from 2.8 to 4.2 MHz are found. For similar sites near calcium cations the experimentally determined values are generally lower and fall between 2.0 and 2.9 MHz. Since the electronegativities of both cations are quite similar, the electric field gradients near these ions are only slightly dependent on the type of ion itself. The quadrupolar coupling products for terminal sites in diopside, which both fall close to the overlap point of the ranges for the two types of cations, tend to support the argument that an average environment is

experienced at these sites. The more noticeable difference is between the bridging and terminal oxygen quadrupolar environments since the field gradients at bridging sites are almost double those at terminal sites.

Finally, from the MAS simulations at the two fields, the values for the asymmetry parameter, η, at each of the three sites in diopside were determined (Table II). This provides additional information above and beyond the coupling product, P_Q. It also allows us to determine with greater precision the value of the actual quadrupolar coupling constants C_Q, giving a quantitative description of the strength the field gradient at each site. Further, all sites in diopside have asymmetry parameters near zero, indicating that the x and y gradients are of approximately the same strength.

In conclusion, we have shown that by performing field-dependent DAS experiments on oxygen-17 in minerals, parameters are obtained which can be directly correlated with structural information. Trends are recognized in the isotropic chemical shifts and the quadrupolar coupling strengths for a series of silicate minerals. It has been demonstrated that these parameters depend on the type of oxygen crystallographic site and the neighboring cation present in the crystals, corroborating extensive earlier studies but further providing information on *all* oxygen sites present in certain complex silicate minerals.

Acknowledgment. We are indebted to J. Stebbins and B. F. Chmelka for preparation of the oxygen-17-enriched silicates. K.T.M. and J.H.B. acknowledge the National Science Foundation for graduate fellowships, and E.W.W. is a NIH postdoctoral fellow. This research was supported by the Director, Office of Energy Research, Office of Basic Energy Sciences, Materials Science Division of the U.S. Department of Energy under Contract No. DE-AC03-76SF00098.

Registry No. Ca_2SiO_4, 10034-77-2; Mg_2SiO_4, 10034-94-3; $CaMgSi_2O_6$, 13774-18-0; $CaSiO_3$, 10101-39-0; $MgSiO_3$, 13776-74-4; larnite, 14284-23-2; forsterite, 15118-03-3; diopside, 14483-19-3; wollastonite, 13983-17-0; clinoenstatite, 14654-06-9; oxygen-17, 13968-48-4.

References and Notes

(1) Deer, W. A.; Howie, P. A.; Zussman, J. *Rock-Forming Minerals*; Halsted Press: New York, 1978.
(2) Breck, D. W. *Zeolite Molecular Sieves: Structure, Chemistry, and Use*; R. E. Krieger: Malabar, FL, 1984.
(3) Bansal, N. P.; Doremus, R. H. *Handbook of Glass Properties*; Academic Press: Orlando, FL, 1986.
(4) Stryer, L. *Biochemistry*, 3rd ed.; W. H. Freeman and Co.: New York, 1988.
(5) Wüthrich, K. *NMR of Proteins and Nucleic Acids*; John Wiley and Sons: New York, 1986.
(6) Timken, H. K. C.; Turner, G. L.; Gilson, J.-P.; Welsh, L. B.; Oldfield, E. *J. Am. Chem. Soc.* **1986**, *108*, 7231–7235.
(7) Timken, H. K. C.; Janes, N. Turner, G. L.; Lambert, S. L.; Welsh, L. B.; Oldfield, E. *J. Am. Chem. Soc.* **1986**, *108*, 7236–7241.
(8) Schramm, S.; Oldfield, E. *J. Am. Chem. Soc.* **1984**, *106*, 2502–2506.
(9) Timken, H. K. C.; Schramm, S. E.; Kirkpatrick, R. J.; Oldfield, E. *J. Phys. Chem.* **1987**, *91*, 1054–1058.
(10) Oldfield, E.; Keniry, M. A.; Shinoda, S.; Schramm, S.; Brown, T. L.; Gutowsky, H. S. *J. Chem. Soc., Chem. Commun.* **1985**, 791–793.
(11) Schramm, S.; Kirkpatrick, R. J.; Oldfield, E. *J. Am. Chem. Soc.* **1983**, *105*, 2483–2485.
(12) Turner, G. L.; Chung, S. E.; Oldfield, E. *J. Magn. Reson.* **1986**, *64*, 316–324.
(13) Walter, T. H.; Oldfield, E. *J. Phys. Chem.* **1989**, *93*, 6744–6751.
(14) Coretsopoulos, C.; Lee, H. C.; Ramli, E.; Reven, L.; Rauchfuss, T. B.; Oldfield, E. *Phys. Rev. B* **1989**, *39*, 781–784.
(15) Takigawa, M.; Hammel, P. C.; Heffner, R. H.; Fisk, Z.; Ott, K. C.; Thompson, J. D. *Phys. Rev. Lett.* **1989**, *63*, 1865–1868.
(16) Li, F.; Brookeman, J. R.; Rigamonti, A.; Scott, T. A. *J. Chem. Phys.* **1981**, *74*, 3120–3130.
(17) Morimoto, K.; Shimomura, K. *J. Phys. Soc. Jpn.* **1984**, *53*, 2752–2760.
(18) Andrew, E. R. *Philos. Trans. R. Soc. London, A* **1981**, *299*, 505–520.
(19) Maricq, M. M.; Waugh, J. S. *J. Chem. Phys.* **1979**, *70*, 3300–3316.
(20) Schaefer, J.; Stejskal, E. O. *J. Am. Chem. Soc.* **1976**, *98*, 1031–1032.
(21) Behrens, H. J.; Schnabel, B. *Physica* **1982**, *B114*, 185–190.
(22) Ganapathy, S.; Schramm, S.; Oldfield, E. *J. Chem. Phys.* **1982**, *77*, 4360–4365.
(23) Lefebvre, F.; Amoureux, J.-P.; Fernandez, C.; Derouane, E. G. *J. Chem. Phys.* **1987**, *86*, 6070–6976.
(24) Amoureux, J. P.; Fernandez, C.; Lefebvre, F. *Mag. Reson. Chem.* **1990**, *28*, 5–10.
(25) Samoson, A.; Lippmaa, E.; Pines, A. *Mol. Phys.* **1988**, *65*, 1013–1018.
(26) Llor, A.; Virlet, J. *Chem. Phys. Lett.* **1988**, *152*, 248–253.
(27) Mueller, K. T.; Sun, B. Q.; Chingas, G. C.; Zwanziger, J. W.; Terao, T.; Pines, A. *J. Magn. Reson.* **1990**, *86*, 470–487.
(28) Mueller, K. T. Ph.D. Thesis; University of California: Berkeley, CA, 1991.
(29) Eastman, M. A.; Grandinetti, P. J.; Lee, Y.; Pines, A. *J. Magn. Reson.* **1992**, *98*, 333–341.
(30) Wu, Y.; Sun, B. Q.; Pines, A.; Samoson, A.; Lippmaa, E. *J. Magn. Reson.* **1990**, *89*, 297–309.
(31) Chmelka, B. F.; Mueller, K. T.; Pines, A.; Stebbins, J.; Wu, Y.; Zwanziger, J. W. *Nature (London)* **1989**, *339*, 42–43.
(32) Mueller, K. T.; Wu, Y.; Chmelka, B. F.; Stebbins, J.; Pines, A. *J. Am. Chem. Soc.* **1991**, *113*, 32–38.
(33) Wu, Y.; Chmelka, B. F.; Pines, A.; Davis, M. E.; Grobet, P. J.; Jacobs, P. A. *Nature (London)* **1990**, *346*, 550–552.
(34) Mueller, K. T.; Chingas, G. C.; Pines, A. *Rev. Sci. Instrum.* **1991**, *62*, 1445–1452.
(35) Jelinek, R.; Chmelka, B. F.; Wu, Y.; Grandinetti, P. J.; Pines, A.; Barrie, P. J.; Klinowski, J. *J. Am. Chem. Soc.* **1991**, *113*, 4097–4101.
(36) Baltisberger, J. H.; Gann, S.; Wooten, E. W.; Chang, T. H.; Mueller, K. T.; Pines, A. *J. Am. Chem. Soc.*, in press.
(37) Chmelka, B. F. Ph.D. Thesis; University of California: Berkeley, CA, 1989.
(38) Warren, B.; Bragg, W. L. *Z. Kristallogr.* **1928**, *69*, 168–193.
(39) Wyckoff, R. W. G. *Crystal Structures*; Interscience: New York, 1948; Vol. 3, Chapter 12, pp. 5–9.
(40) Morimoto, N.; Appleman, D. E.; Evans, H. T., Jr. *Z. Kristallogr.* **1960**, *114*, 120–147.
(41) Troger, F. J. *Z. Kristallogr.* **1968**, *127*, 291–308.
(42) Midgely, C. M. *Acta Crystallogr.* **1952**, *5*, 307–312.
(43) Schmidt, V. H. *Proc. Ampère Intl. Summer School II* **1971**, 75.
(44) Man, P. P.; Klinowski, J.; Trokiner, A.; Zanni, H.; Papon, P. *Chem. Phys. Lett.* **1988**, *151*, 143–150.
(45) Alderman, D. W.; Solum, M. S.; Grant, D. M. *J. Chem. Phys.* **1986**, *84*, 3717–3725.
(46) Press, W. H.; Flannery, B. P.; Teukolsky, S. A.; Vetterling, W. T. *Numerical Recipes. The Art of Scientific Computing*; Cambridge University Press: Cambridge, 1986.
(47) Mueller, K. T.; Wooten, E. W.; Pines, A. *J. Magn. Reson.* **1991**, *92*, 620–627.
(48) Kintzinger, J.-P. In *NMR: Basic Principles and Progress*; Diehl, P., Fluck, E., Kosfeld, R., Eds.; Springer-Verlag: Berlin, 1978.
(49) Kirkpatrick, R. J. *Rev. Minerol.* **1988**, *18*, 341–403.